

# Excitonic Effects on the Optical Response of Graphene and Bilayer Graphene

Li Yang, Jack Deslippe, Cheol-Hwan Park, Marvin L. Cohen, and Steven G. Louie

Department of Physics, University of California at Berkeley, California 94720 and  
Materials Sciences Division, Lawrence Berkeley National Laboratory, Berkeley,  
California 94720

## Abstract:

We present first-principles calculations of many-body effects on the optical response of graphene and bilayer graphene employing the GW-Bethe Salpeter equation approach. We find that because of electron-hole interactions, resonant excitons are formed in these two-dimensional semimetals. These give rise to a prominent peak in the absorption spectrum near 4.5 eV with a different lineshape and significantly red-shifted peak position from those of an absorption peak arising from inter-subband transitions in an independent quasiparticle picture. In the infrared-frequency regime, our calculated optical absorbance per graphene layer is approximately a constant, 2.4%, in good agreement with recent experiments; additional low frequency features are found for bilayer graphene owing to its band structure.

Excitonic (electron-hole interaction) effects are observable in the optical response of semiconductors, however, they are typically unimportant in that of conventional bulk metals because of the strong screening of these interactions from free carriers. However, recent first-principles calculations [1, 2] have predicted, and subsequent experimental studies [3] have confirmed, the existence of bound excitons in one-dimensional metallic carbon nanotubes. Therefore, it is of considerable interest to explore whether there are significant excitonic effects in two-dimensional metallic or semi-metallic systems.

Graphene is an appropriate system to examine because it is a two-dimensional semimetal [4-6], which has generated considerable interest because of the interesting physics associated with its unusual electronic structure and its promising device applications [7]. In particular, the optical properties of graphene display many intriguing features, such as a constant optical conductivity in the infrared-frequency regime, gate-dependence optical absorbance, and a unique magneto-optical spectrum [8-10]. However, there have been no first-principles studies to date of the optical properties of graphene including excitonic effects that are known to be extremely important in reduced dimensional materials.

In this work, we have carried out first-principles calculations using many-body Green's function theory to study the excitonic effects on the optical spectra and, in particular, the absorbance of graphene and bilayer graphene. Following the approach of Rohlfing and Louie [11], we calculate the optical response of isolated single and bilayer intrinsic graphene sheets in three stages: (i) we obtain the electronic ground state using density functional theory (DFT) within the local density approximation (LDA); (ii) the quasiparticle energies are calculated within the GW approximation to the electron self energy [12]; and (iii) we solve the Bethe-Salpeter equation (BSE) of the two-particle Green's function to obtain the photo-excited states and optical absorption spectrum [11].

Our first-principles results show that there is a significant self-energy correction to the band velocity of the Dirac quasiparticles in agreement with previous first-principles studies [16, 17]. The absorption peak arising from the subband transitions near the M-point van Hove singularity at around 5.0 eV is totally suppressed and replaced by a new peak at 4.5 eV with a different lineshape owing to electron-hole interactions. Our analysis shows that, in graphene, a two-dimensional semimetal, this change in optical spectrum is the result of a redistribution of optical transition strengths by strongly resonant excitons. Moreover, we explicitly show that the infrared spectral absorbance per graphene layer including electron-hole interactions is approximately a constant, 2.4%, in excellent agreement with recent experiments [13, 14].

In our studies, the intra-layer structure of graphene and bilayer graphene is fully relaxed using the calculated forces and stress on the atoms within DFT/LDA. For Bernal-stacked bilayer graphene, the inter-layer distance is chosen to be the experimental value of graphite (0.334 nm). The calculations are done in a supercell arrangement [30] with a plane-wave basis using norm-conserving pseudopotentials [15] with a 60 Ry energy

cutoff. The vacuum distance between graphene sheets in neighboring supercells is 1.2 nm to avoid spurious interaction effects. A  $32 \times 32 \times 1$  uniform k-point sampling grid is used to ensure converged LDA results. In calculating the quasiparticle energies, a  $64 \times 64 \times 1$  k-point grid is necessary for computing the converged self energy within the GW approximation. We take into account dynamical screening effects through the generalized plasmon pole model [12]. In solving the BSE, the electron-hole interaction kernel is evaluated first on a coarse k-grid ( $64 \times 64 \times 1$ ) and then interpolated onto a fine grid ( $200 \times 200 \times 1$ ) to obtain converged exciton states and optical spectra [11]. Two valence bands and two conduction bands are included for calculating the optical absorption spectra up to 7.0 eV. In the discussion below, we shall focus on the absorption spectrum for light polarized parallel to the graphene plane.

The LDA Kohn-Sham eigenvalues and the GW quasiparticle band structure of graphene are shown in Fig. 1 (a), and magnified around the Dirac point in Fig. 1 (b). The Fermi velocity is significantly increased by the self-energy correction. While the LDA Fermi velocity is  $0.85 \times 10^6$  m/s, the GW value is  $1.15 \times 10^6$  m/s that is in good agreement with experiment [6], as well as with previous GW calculations [16, 17]. In addition to many-electron effects, it has to be pointed out that substrate effects and electron-phonon interactions also play important roles in determining the details of the experimentally measured band structure around the Dirac point [18-20]. The LDA and quasiparticle band structures of bilayer graphene are shown in Fig. 2. In addition to the overall band width increase, the separation between parallel bands at the K point increases because of many-body interactions as shown in Fig. 2 (b). For example, the separation between the highest and the second highest valence bands increases from 320 meV (LDA) to 410 meV (GW), a 28% correction.

Fig. 3 (a) shows the calculated optical spectrum of graphene with and without the electron-hole interaction included. The plotted quantity  $\alpha_2(\omega)$  is the imaginary part of the polarizability per unit area and is obtained by multiplying the calculated dielectric susceptibility,  $\chi = (\epsilon - 1)/4\pi$ , by the distance between adjacent graphene layers (or bilayers) in our supercell arrangement. This quantity  $\alpha_2(\omega)$  when multiplied by the area of graphene or bilayer graphene gives the polarizability of the system. The absorption below 0.3 eV is not shown in Fig. 3 (a) because intraband transitions and temperature effects are important there and our calculation does not include these factors. The interband transitions between  $\pi$  electronic states dominate the spectrum up to 7 eV. In the absence of the electron-hole interaction, the interband transitions between the highest valence band and the lowest conduction band around the M point form a prominent absorption peak at 5.2 eV. However, with excitonic effects included, the prominent absorption peak is now at 4.6 eV which is a 600 meV shift. In addition, as seen in Fig. 3 (a), the peak profile is substantially modified from an almost symmetric peak for the interband transitions case to an asymmetric one for the case when electron-hole interactions are included. This provides a possible way for measurements to distinguish between the two cases.

It is surprising to find such large excitonic effects (an apparent shift of 600 meV of feature in the optical spectrum) in this two-dimensional semimetal, given the fact that the

binding energy found in one-dimensional metallic carbon nanotubes is only tens of meV, and there is no significant excitonic effect in bulk metals. In Fig. 3 (b), we have plotted both the joint density states of quasiparticles from the GW calculation and the density of excitonic states from solving the BSE. It is clear that these two curves are nearly identical to each other, similar to findings in bulk silicon and gallium arsenide [11].

To analyze our results, we rewrite the relevant optical transition matrix element for going from the ground state  $|0\rangle$  to a correlated electron-hole (exciton) state

$$|i\rangle = \sum_{ks} \sum_v^{hole} \sum_c^{elec} A_{vck}^i |vck\rangle \text{ into the form [11]}$$

$$\langle 0|\bar{v}|i\rangle = \sum_v \sum_c \sum_k A_{vck}^i \langle vk|\bar{v}|ck\rangle = \int S_i(\omega) d\omega,$$

where

$$S_i(\omega) = \sum_v \sum_c \sum_k A_{vck}^i \langle vk|\bar{v}|ck\rangle \delta(\omega - (E_{ck} - E_{vk}))$$

which gives a measure of the contribution of all interband pairs  $(ck, vk)$  at a given transition energy  $\omega$  to the optical transition strength of the exciton state  $i$ .

In Fig. 4, we have plotted histograms of the function  $S_i(\omega)$  and its integrated value up to given frequency for three bright optically excited state of graphene obtained using the BSE. The goal is to provide an understanding to why excitonic effects enhance the absorption around 4.5 eV but depress it around 5.1 eV. In Fig. 4 (a), the state for which  $S_i(\omega)$  is plotted has an energy of 1.6 eV. Since there is almost no excitonic effect for the optical spectrum below 2.0 eV, this state displays a very narrow energy distribution of in  $S_i(\omega)$ , as expected. In Fig. 4 (b) and (c), the states studied, located around 4.5 eV and 5.1 eV, respectively, show a considerably wide energy distribution in  $S_i(\omega)$ , indicating that the states are linear combinations of many free electron-hole pair configurations of different energies which is consistent with the fact that there are significant excitonic effects in this energy regime.

Furthermore, in Fig. 4 (b), an important feature about this excitonic state is that its optical transition matrix element distribution becomes asymmetric with larger amplitude extending to the high-energy direction. Also since the running integrated value of  $S_i(\omega)$  in Fig. 4 (b) increases significantly from 4.5 eV to 5.5 eV which is exactly the range of the strong interband absorption peak, it is clear that this particular resonant exciton steals optical transition strength from the prominent interband absorption peak around 5.1 eV and enhances the optical absorption around 4.5 eV. In contrast, the  $S_i(\omega)$  for the state shown in Fig. 4 (c) is more anti-symmetric than that shown in (b). The negative and positive contributions above and below 5.1 eV, respectively, nearly cancel each other and the final integrated strength is only one third of that for the exciton in (b). As a result, the optical absorption around 5.1 eV is depressed. Thus, similar to one-dimensional carbon nanostructures such as metallic carbon nanotubes [1, 2] and semiconducting graphene

nanoribbons (GNRs) [21], excitonic states dominate the optical absorption spectra in the energy region from 4 to 5 eV in graphene.

The optical absorbance of graphene is expected to be a constant (2.29%) in the infrared spectral range [10, 13, 14, 22-28]. In Fig. 3 (c), we present the calculated optical absorbance,  $A(\omega) = \frac{4\pi\omega}{c} \alpha_2(\omega)$ , of graphene with and without many-body effects included. Our calculated absorbance per graphene layer is nearly the same (2.4%) with and without electron-hole interaction included. This first-principles result is in good agreement with measured values and is consistent with previous single-particle studies and with model calculation with many-electron effects included [29].

The imaginary part of the polarizability and the absorbance of bilayer graphene calculated with and without electron-hole interaction included are presented in Fig. 5 (a), showing similar excitonic effects as those in single-layer graphene, with a significant apparent red-shift in the position of the prominent absorption peak around 5 eV. There is also a noticeable absorption feature at 0.4 eV, contributed by interband transitions near the Dirac point (from the highest valence band to the second lowest conduction band and from the second highest valence band to the lowest conduction band). Moreover, in Fig. 5 (b), the infrared spectral absorbance for low-energy absorption is around 4.8%, which is almost exactly twice that of single-layer graphene (2.4%), and this result is in good agreement with the experiment [13].

The large excitonic effects found in bilayer graphene have similar origins to those in graphene. However, as shown in Fig. 2 (b), the conduction band and valence band in the bilayer case touch each other and they have parabolic shape. This provides a larger DOS around the Fermi level and results in stronger screening than that of intrinsic single-layer graphene. Therefore, as shown in Fig. 5, an apparent 450 meV red-shift of the prominent absorption peak of bilayer graphene is obtained with the inclusion of the electron-hole interaction, which is smaller than that of single-layer graphene (600 meV).

In conclusion, we have performed first-principles calculations on the quasiparticle energies and optical properties of single- and bi-layer graphene with many-electron effects included. A substantial renormalization of the Fermi velocity of graphene is obtained in our GW calculations. Resonant excitonic effects in graphene and bilayer graphene result in significant changes in the optical absorption spectrum in the energy regime corresponding to the subband electronic transitions near the van Hove singularity as compared to the independent-particle picture. Finally, we have directly shown that excitonic effects do not change the optical absorbance per graphene layer in the infrared range from that calculated within the single-particle picture, in agreement with experimental findings.

We thank Y.-W. Son, D. Prendergast and E. Kioupakis for discussions. This research was supported by NSF Grant No. DMR04-39768 and by the Director, Office of Science, Office of Basic Energy under Contract No. DE-AC02-05CH11231. Jack Deslippe acknowledges the funding from the DOE Computational Science Graduate Fellowship

(CSGF) under grant number DE-FG02-97ER25308. Computational resources have been provided by Lonestar of teragrid at the Texas Advanced Computing Center (TACC) of the University of Texas at Austin.

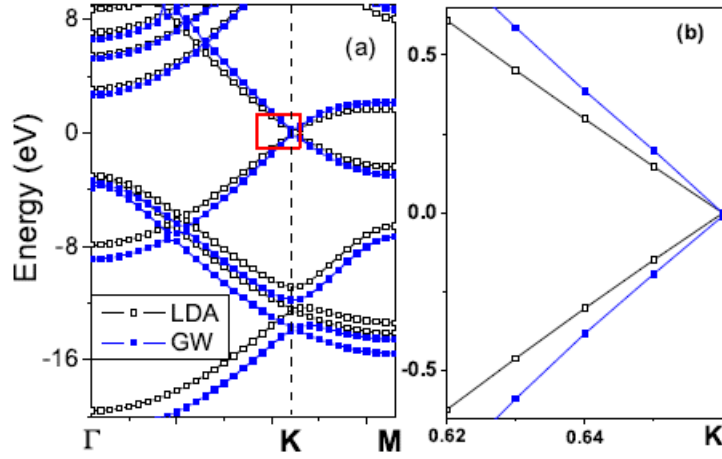


Fig. 1 (color online) Band structure of graphene. (a) LDA Kohn-Sham eigenvalues and GW quasiparticle band structures. (b) A magnification of band structures close the Dirac point (K). The wavevector is in units of  $\frac{2\pi}{a}$ , where  $a$  is the in-plane lattice constant of graphene.

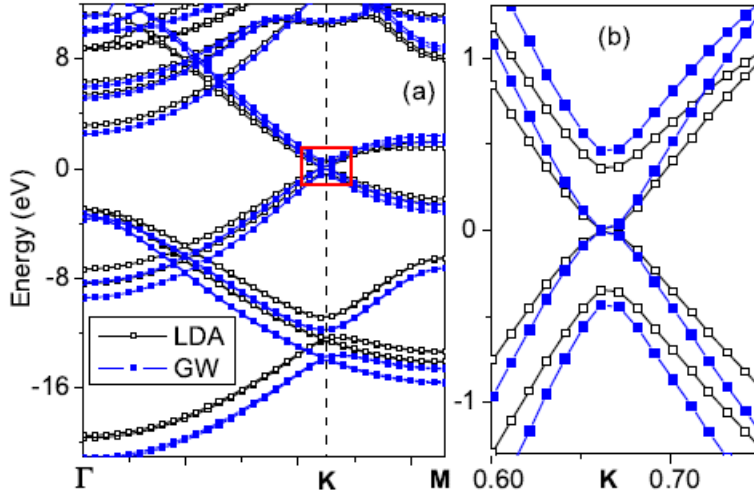


Fig. 2 (color online) Band structure of bilayer graphene. (a) LDA Kohn-Sham eigenvalues and GW quasiparticle band structures. (b) A magnification of the band structures close to the Dirac point (K). The wavevector is in units of  $\frac{2\pi}{a}$ , where  $a$  is the in-plane lattice constant of bilayer graphene.

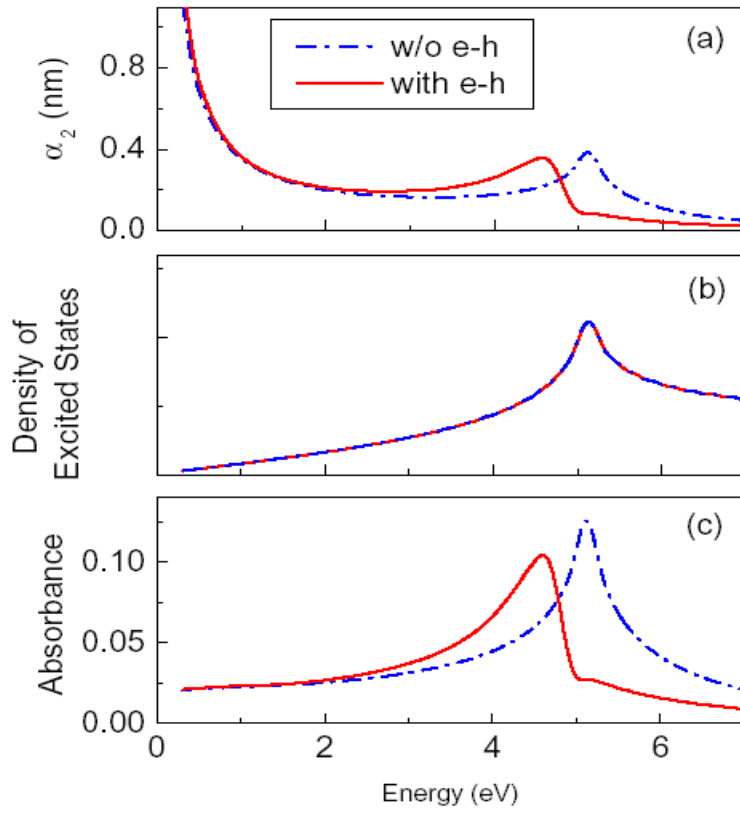


Fig. 3 (color online) (a) Optical absorption spectra, (b) density of excited states, and (c) absorbance of graphene with and without excitonic effects included. A Lorentzian broadening of width of 0.05 eV is applied.

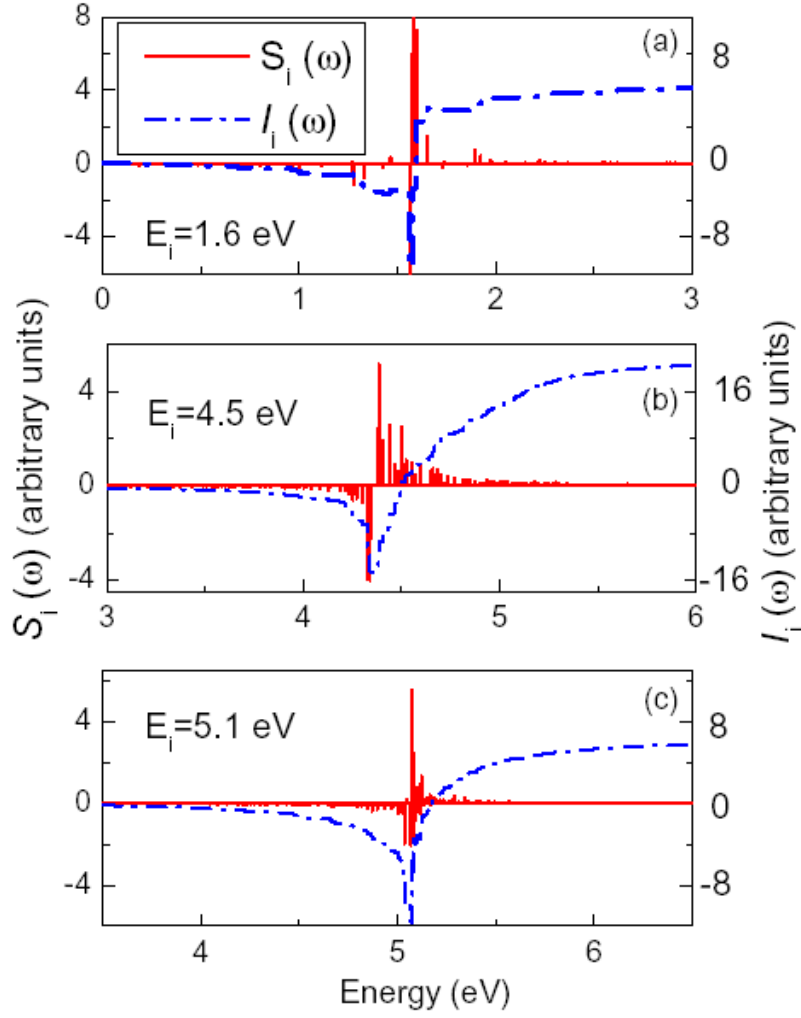


Fig. 4 (color online) Histograms of  $S_i(\omega)$  and the corresponding integration  $I(\omega) = \int_0^\omega S(\omega') d\omega'$  of three typical bright eigenstates determined from solving the BSE for graphene. Please note that the right scale of (b) is twice times larger than that of (a) and (c).

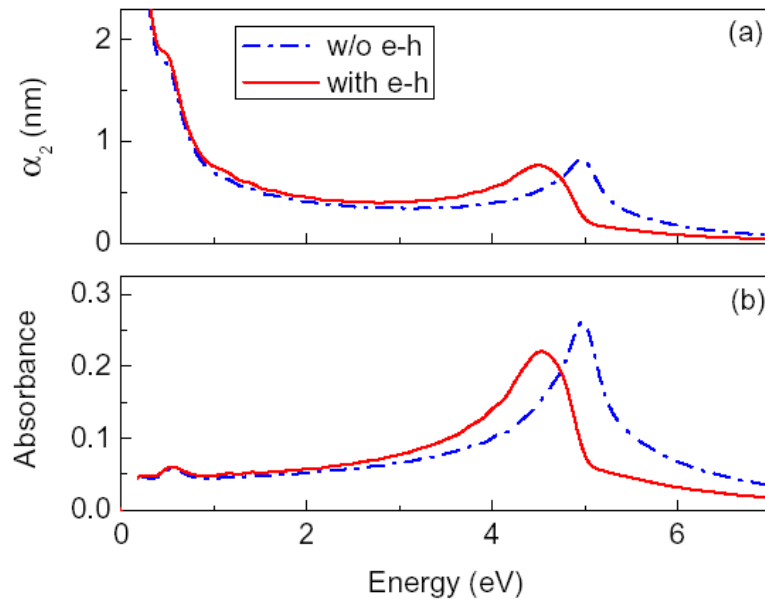


Fig. 5 (color online) (a) Optical absorption spectra and (b) absorbance of bilayer graphene with and without excitonic effects included. A Lorentzian broadening with width of 0.05 eV is applied.

## References:

- [1] C. D. Spataru, S. Ismail-Beigi, L. X. Benedict, and Steven G. Louie, Phys. Rev. Lett. 92, 077402 (2004).
- [2] J. Deslippe, C. D. Spataru, D. Prendergast, and S. G. Louie, Nano Lett 7, 1626 (2007).
- [3] Feng Wang et al., Phys. Rev. Lett. 99, 227401 (2007).
- [4] K. S. Novoselov et al., Science 306, 666 (2004).
- [5] K. S. Novoselov et al., Nature (London) 438, 197 (2005).
- [6] Y. Zhang, Y.-W. Tan, H. L. Stormer, P. Kim, Nature 438, 201 (2005).
- [7] A. K. Geim and K. S. Novoselov, Nature Materials 6, 183 (2007); A. H. Castro Neto, et al., Rev. Mod. Phys. 81, 109 (2009), and references therein.
- [8] F. Wang, et al., Science 320, 206 (2008).
- [9] D. S. L. Abergel and Vladimir I. Fal'ko, Rev. B 75, 155430, (2007).
- [10] V.P. Gusynin and S.G. Sharapov, Phys. Rev. B 73, 245411, (2006).
- [11] M. Rohlfing and S. G. Louie, Phys. Rev. B 62, 4927 (2000).
- [12] M.S. Hybertsen and S.G. Louie, Phys. Rev. B 34, 5390 (1986).
- [13] R. R. Nair, et al., Science 320, 1308 (2008).
- [14] K.F. Mak, et al., Phys. Rev. Lett. 101, 196405, 2008.
- [15] N. Troullier and J.L. Martins, Phys. Rev. B 43, 1993 (1991).
- [16] P.E. Trevisanutto, et al., Phys. Rev. Lett. 101, 226405 (2008).
- [17] C. Attaccalite, A. Greneis, T. Pichler, A. Rubio, arXiv:0808.0786v2.
- [18] S.Y. Zhou, et al., Nature Materials 6, 770 (2007).
- [19] A. Bostwick, et al., Nature Physics 3, 36 (2007).
- [20] C.-H. Park, F. Giustino, M.L. Cohen, and S.G. Louie, Phys. Rev. Lett. 99, 086804 (2007); M. Calandra and F. Mauri, Phys. Rev. B 76, 205411 (2007); Tse, Hu, and Das Sarma, Phys. Rev. Lett. 101, 066401 (2008).

- [21] L. Yang, M. L. Cohen and S. G. Louie, Nano Lett 7, 3112 (2007); D. Prezzi, et al., Phys. Rev. B 77, 041404(R) (2008).
- [22] E. J. Nicol and J. P. Carbotte, Phys. Rev. B 77, 155409 (2008).
- [23] J.M. Dawlaty, et al., arXiv:cond-mat/08013302.
- [24] T. Stauber, N. M. R. Peres and A. K. Geim, Phys. Rev. B 78, 085432 (2008).
- [25] T. Ando, Y. S. Zheng, and H. Suzuura, J. Phys. Soc. Jpn. 71, 1318 (2002).
- [26] C. Zhang, L. Chen and Z. Ma, Phys. Rev. B 77, 241402 (2008).
- [27] Z. Q. Li, et al., arXiv:cond-mat/08073776.
- [28] N. M. R. Peres, F. Guinea, and A. H. Castro Neto, Phys. Rev. B 73, 125411 (2006).
- [29] M. I. Katsnelson, Europhys Lett. 84, 37001 (2008).
- [30] M.L. Cohen, M. Schlüter, J.R. Chelikowsky, and S.G. Louie, Phys. Rev. B 12, 5575 (1975).